12-2005

Sensors to Monitor CFRP/Concrete Bond in Beams Using Electrochemical Impedance Spectroscopy

Sangdo Hong
Indiana Department of Transportation

Ronald S. Harichandran
University of New Haven, rharichandran@newhaven.edu

Publisher Citation

Hong, S., and Harichandran, R. S. (2005). "Sensors to monitor CFRP/concrete bond in beams using electrochemical impedance spectroscopy." Journal of Composites for Construction, ASCE, 9(6), 515-523. doi:10.1061/(ASCE)1090-0268(2005)9:6(515)

Comments

This is the authors' accepted version of the article published in *Journal of Composites for Construction.* The version of record can be found in the ASCE library at
http://dx.doi.org/10.1061/(ASCE)1090-0268(2005)9:6(515)

Sensors to Monitor CFRP/Concrete Bond in Beams Using Electrochemical Impedance Spectroscopy

Sangdo Hong[1] and Ronald S. Harichandran,[2] P.E., Member, ASCE

ABSTRACT

The use of inexpensive electrochemical impedance spectroscopy based sensor technology for NDE of bond degradation between external CFRP reinforcement and concrete is examined. Copper tape on the surface of the CFRP sheet, stainless steel wire embedded in the concrete, and reinforcing bars were used as the sensing elements. Laboratory experiments were designed to test the capability of the sensors to detect the debonding of the CFRP from the concrete and to study the effect of short-term (humidity and temperature fluctuations) and long-term (freeze-thaw and wet-dry exposure, and rebar corrosion) environmental conditions on the measurements. The CFRP sheet was debonded from the concrete and impedance measurements were taken between various pairs of electrodes at various interfacial crack lengths. The dependence of the impedance spectra, and of the parameters obtained from equivalent circuit analysis, on the interfacial crack length was studied. Capacitance parameters in the equivalent circuit correlated strongly with the interfacial crack length and can be used to assess the global state of the bond between CFRP sheets and concrete. Impedance measurements taken between embedded wire sensors can be used to detect the location of debonded regions.

[1] Former Graduate student, Dept. of Civil & Envir. Engrg., Michigan State Univ., East Lansing, MI 48824-1224

[2] Professor and Chair, Dept. of Civil & Envir. Engrg., Michigan State Univ., East Lansing, MI 48824-1224; Tel.: 517-355-5107; Fax: 517-432-1827; E-Mail: harichan@egr.msu.edu

Introduction

Many structures built in the past need strengthening and retrofitting to overcome deficiencies caused by increased load demands, environmental deterioration and structural aging. Thirty-five percent of all bridges in the U.S. are estimated to be structurally deficient and require repair, strengthening, widening or replacement (Karbhari and Zhao 2000). To overcome structural deficiencies, composite materials such as fiber-reinforced polymers (FRP) are being increasingly used for strengthening and retrofitting. Carbon fiber reinforced polymer (CFRP) is a well-known high performance composite material used to strengthen reinforced concrete structural components.

Concrete beams strengthened or retrofitted with FRP behave as composite components, and their strengths are calculated by taking this into account. Interfacial bonding between the FRP and concrete plays a significant role in achieving composite behavior and increasing strength. For flexural strengthening of beams, CFRP plates or sheets are bonded to the tension face—a simple and convenient technique (Rahimi and Hutchinson 2001). Unlike steel plates, FRP plates do not suffer from corrosion problems. However, the interfacial bond between the FRP and concrete can deteriorate due to environmental and load-related issues leading to debonding.

Concrete structures with FRP plates can exhibit a brittle failure mode if the FRP debonds from the concrete. Debonding of the plates and ripping of concrete are common failure modes (Nguyen et al. 2001) initiated due to highly localized stress concentration in the interface layer (Buyukozturk and Hearing 1998). It is therefore important to identify the integrity of the interfacial bond between concrete and the FRP using effective nondestructive evaluation (NDE) techniques.

Visual inspection is not a reliable method of assessing the integrity of interfacial bond in composite components. “Tap” tests are time consuming and difficult to conduct in structural components that are difficult to access. Destructive tests are not feasible for in-service structures. Different NDE methods, including ultrasonic (e.g., Mirmiran and Wei 2001) and microwave techniques (e.g., Akuthota et al. 2004), have been used to detect or monitor the delamination between two composite materials. However, these NDE methods do not always work well for concrete structures rehabilitated with FRP, and some are quite complicated to use in the field. It is important to develop inexpensive, simple and effective NDE methods for concrete structures rehabilitated with FRP.

Background Concepts on EIS

Traditionally, electrochemical impedance spectroscopy (EIS) has been used to detect coating deterioration and substrate corrosion, and the EIS technique is performed in an electrolyte with working, counter and reference electrodes (Kendig and Scully 1989). Use of an external electrolyte is cumbersome in the field. However, it is possible to use *in-situ* electrodes to measure the impedance in the ambient condition without submerging the electrochemical cell (Davis et al. 2000). In this modified EIS technique, the reference and working electrodes are combined into a single electrode, and yield stable measurements.

In-situ sensors have been used to detect moisture ingress and crack propagation in structural adhesive bonds (Davis et al. 2000). This sensor technology uses EIS to inspect the integrity of the bond. The impedance typically increases in magnitude as the crack propagates (Davis et al. 1999). In the simplest method for detecting debonding, the impedance spectra can be compared directly (Hong 2003). A raw impedance analysis is quick and the investigator performing analysis does not need to be highly trained. However, additional information can be obtained from the

impedance spectra by using equivalent circuit analysis. Davis et al. (1999) found that the resistive components in the equivalent circuit they used were functions of moisture content and the capacitance parameter was a function of both moisture content and bonded area.

Electrical Impedance

Electrochemical impedance is the resistance to current in an electrochemical cell. It is generally obtained by measuring the AC current across a pair of electrodes due to an applied AC voltage. Electrical resistance is independent of the frequency of the harmonic (sinusoidal) AC voltage excitation. However, electrical impedance is often dependent on frequency. When the excitation signal is harmonic, the response signal is also harmonic at the same frequency with an amplitude and phase angle. The impedance, Z, is a complex-valued quantity and is defined as the ratio between the excitation voltage, $V(t)$, and the response current, $I(t)$:

$$Z = \frac{V(t)}{I(t)} \tag{1}$$

For a harmonic AC excitation signal, $V(t)$ may be expressed as

$$V(t) = V_o(\cos\omega t + j\sin\omega t) \tag{2}$$

where ω is the circular natural frequency of the applied voltage (expressed in radian/second), V_0 is the amplitude of the excitation signal and j is the unit imaginary number. The harmonic current response $I(t)$ may be expressed as

$$I(t) = I_o[\cos(\omega t - \phi) + j\sin(\omega t - \phi)] \tag{3}$$

where I_0 is the amplitude of the harmonic current and ϕ is the phase shift. The electrical impedance in Eq. (1) is then

$$Z = Z_o(\cos\phi + j\sin\phi) \tag{4}$$

where $Z_0 = V_0/I_0$ is the magnitude of the impedance. Both the magnitude and phase vary with the excitation frequency and it is common to display the impedance by plotting the variation of its magnitude and phase with excitation frequency. The plot of the magnitude vs. excitation frequency is called the Bode magnitude plot (or magnitude spectrum), and the plot of the phase vs. excitation frequency is called the phase spectrum.

Impedance, Z, is generally complex-valued. The impedance of a resistor, R, is $Z_R = R$ and is real-valued. The impedance of a capacitor, C, is purely imaginary and is $Z_C = 1/(j\omega C)$. The constant phase element (CPE) is often used in an equivalent circuit to represent the response of real-world electrochemical systems. These systems do not respond ideally because some properties are not homogeneous and often there are distributed elements in addition to lumped elements in the system. The impedance of the CPE is

$$Z_{CPE} = A(j\omega)^{-\alpha} \tag{5}$$

When $\alpha = 1$ (maximum value), the CPE is equivalent to a capacitor with $A = 1/C$ (the inverse of the capacitance), and when $\alpha = 0$ (minimum value), the CPE is equivalent to a resistor with $A = R$.

The capacitance between two parallel plates separated by a dielectric material may be expressed as

$$C = \frac{\varepsilon\varepsilon_0 A}{d} \tag{6}$$

where ε_0 = electrical permittivity, ε = relative electrical permittivity, A = area of the plates, and d = distance between the plates. While the value of ε_0 is constant, the value of ε depends on the

dielectric material. Moisture in the dielectric material changes the value of ε. Davis et al. (1999) used Equation (6) to evaluate the moisture uptake into the adhesive in a metal-FRP bond.

EIS and Equivalent Circuit Analysis

In EIS, an AC voltage is applied between the working and counter electrodes. The complex impedance spectrum is then measured as a function of frequency. Two methods of analyzing the impedance spectra from a set of measurements are common. The first method is to simply compare the raw impedance spectra. The impedance spectrum can be plotted in different ways. The conventional presentations are the Bode magnitude and phase plot, Nyquist plot, and real and imaginary impedance plots. The impedance spectra are compared over the entire frequency range or over specific frequencies. The second method is to analyze the impedance spectra by using a lumped parameter equivalent circuit model. In this method, the parameters of an electrical circuit which has a theoretical impedance similar to that of the measured impedance are estimated, and spectra are compared based on the differences in the estimated parameters. The equivalent circuit used in this research is shown in Figure 1(a). The circuit consists of a loop that is composed of a resistance, capacitance and a constant phase element (CPE), and two simple resistor/capacitor loops in series.

A justification for the equivalent circuit used is an understanding of the physical process of current flow. Figure 1(b) shows the charge transfer process in a CFRP-strengthened reinforced concrete beam with the rebar and the CFRP used as electrodes. Charge transfer between ions and the electrode involves long-range electrostatic forces, so that their interaction is essentially independent of the chemical properties of ions. Charge transfer through the electrolyte (pore fluid in the case of concrete) occurs by the diffusion of ions. At low excitation frequencies, the impedance to current flow is controlled by the rate of diffusion, while at high frequencies, the imped-

ance is controlled by the kinetics of the charge transfer processes at the electrode/electrolyte interface. In Figure 1(a) the loops containing the resistance and capacitance in the equivalent circuit represent the double layer effects at the two electrodes, and the loop with the CPE element represents the body of concrete.

Several simpler circuits were tried before arriving at the one that was used (Hong 2003). A simple Randles cell and the circuit commonly used when examining failed coatings (Gamry 2005, Davis 2000) were among those that were tried. None of the simpler circuits were able to provide a good fit for the variety of impedance spectra obtained in this work with the various combinations of sensors. While the equivalent circuit used has eight parameters, electrochemical systems such as the one in this work that are governed by mixed kinetic and diffusion control are often modeled with circuits that have nine parameters (Gamry 2005).

Experimental Setup and Procedures

Concrete structures rehabilitated with CFRP are subjected to various short- and long-term environmental conditions. Short-term environmental conditions include the variation of temperature and humidity. Long-term environmental conditions include freeze-thaw cycles, wet- dry cycles and corrosion of the rebar. The effect of rebar corrosion on the measured impedance spectra was studied because the potential of using the rebar as an electrode was investigated. The variability in measured impedance due to short- and long-term environmental effects must be understood if the measurements are to be used to detect debonding of CFRP from concrete.

Experimental Setup

The study on detection of CFRP debonding was conducted with medium-sized reinforced concrete specimens with dimensions of 150×150×600 mm and a large reinforced concrete beam with dimensions of 600×450×2400 mm. The study on the effects of environmental conditions

was conducted with small reinforced concrete specimens with dimensions of 150×150×300mm. Some specimens were manufactured with chloride (11.0 kg NaCl per cubic meter of concrete) and some without chloride. The CFRP was bonded over the entire width of each specimen. The CFRP was provided by Master Builders and had a nominal tensile strength of 700 N/mm of width. The concrete had a compressive strength of 35.7 MPa (5180 psi) after 28 days of curing. The test specimens were prepared with an initial crack by using a Teflon insert. To propagate the interfacial crack between the CFRP layer and the concrete substrate, a wedge (sharpened saw blade) was driven with a hammer. The position of the front edge of the saw blade after it was driven was taken as the leading edge of the crack. The wedge test on the large beam was conducted at ambient conditions with temperatures varying from 18^{o}C to 24^{o}C and relative humidity varying from 30% to 60%. The relative humidity was measured using a humidity meter. None of the specimens had any external load applied to them and were supported on a table or floor over their entire length. The number of each type of specimen used is shown in Table 1. The sensor (electrode) arrangement for the medium-sized specimens is shown in Figure 2. The C_i sensors consisted of copper tape with a conductive adhesive mounted directly on the outside surface of the CFRP before any epoxy was applied. The W_i sensors consisted of stainless steel wire set into grooves on the concrete specimen before the CFRP was bonded. The W_7 wire sensor in the longitudinal direction crosses the lateral wire sensors and was therefore electrically isolated from those by using a small shrink wrap tube at each intersection point. R represents a reinforcing bar (rebar).

Experimental Procedure

Different sensor combinations were used to produce impedance spectra. Combinations of internal sensors (Wi) to external sensor (C_i), rebar (R) to external sensors, and pairs of internal

sensors were used to produce the impedance spectra at different crack states. The impedance spectra were obtained over the frequency range from 0.1 Hz to 100 kHz using a commercial potentiostat and software marketed by Gamry Instruments, Inc. The potentiostat is constructed on a PC card and is inserted into a computer for use. The impedance measurements between a given pair of sensors were stable and repeatable at a given time. Once the raw impedance data was obtained, comparisons of measured spectra and equivalent circuit analysis were performed. The measured impedances were compared over the entire frequency range and also at specific frequencies. Equivalent circuit analysis adjusts the parameters of the circuit shown in Figure 1 using a nonlinear least squares algorithm such that the impedance of the circuit closely matches the data. Equivalent circuit analysis was performed using computer software marketed by Gamry Instruments (Gamry 2003). Figure 3 shows typical impedance magnitude and phase spectra measured from the rebar to an external sensor and the impedance of the fitted equivalent circuit. Because the CFRP is highly conductive, the entire sheet acts as a single electrode and measurements from the rebar to any of the external sensors yielded essentially the same measurements.

Experimental Results

Parameters of the Equivalent Circuit

The elements in the equivalent circuit in Figure 1 control the behavior of the fitted impedance spectrum over different frequency ranges. The impedance measurements shown in Figure 3 are characteristic of an electrochemical system governed by mixed kinetic and diffusion control. The C1 (capacitance), R1 (resistance) and CPE (constant phase element) parameters control the fitted impedance spectrum in the low-frequency region and characterize the diffusion process in the electrolyte (pore fluid in the concrete). The C2, C3, R2 and R3 parameters control the fitted

impedance spectrum in the mid- to high-frequency region and characterize the kinetics of the charge transfer processes at the electrode-electrolyte (steel/concrete and CFRP/concrete) interfaces. The high-, mid- and low-frequency regions are defined as 1000-100,000 Hz, 10-1000 Hz and 0.1-10 Hz, respectively.

No major problems were encountered in fitting the equivalent circuit parameters to the measurements using the Gamry software. Initial values specified for each parameter are shown in Table 1.

Effect of CFRP Debonding

Investigation of the debonding of CFRP reinforcement from concrete was conducted using the wedge test in two different environmental conditions with medium-sized and large concrete specimens. One condition was a controlled environment with a temperature of about 5^{o}C and a relative humidity range of about 35 to 40%. The other condition was an ambient environment with a temperature of about 22^{o}C and variable humidity. For medium-sized specimens, impedance measurements were made from the rebar to each of the copper tape sensors and between pairs of internal wire sensors. The large beam had four rebars (two at the top and two at the bottom) and stirrups (vertical steel), and measurements were taken from one of the rebars closest to the CFRP sheet and the external sensors and between pairs of internal wire sensors. Equivalent circuit analysis was performed for all impedance measurements. Impedance measurements taken from the reinforcing bar (R) to any of the copper tape sensors (C_i) were essentially identical. This observation implies that the highly conductive CFRP serves as a single continuous electrode even at this large scale. As a result, each equivalent circuit parameter value corresponding to the impedance measurement from the rebar sensor to each external copper tape sensor was averaged at each crack state.

Assessing the Global State of the Bond

Impedances were measured for three medium concrete specimens in a refrigerator and three medium specimens in the ambient condition at the initial crack state (100mm crack length). The cracks were then extended in the same environmental conditions and additional readings were taken. The refrigerator provided a controlled environment with a temperature of about 5^{o}C and a relative humidity range between 35 and 40%. For the ambient condition, the temperature fluctuated between 18^{o}C and 24^{o}C and the relative humidity fluctuated between 30% and 60%. The debonding was best detected with impedance measurements from the rebar to the copper tape sensors.

Typical variations of the impedance spectra as the crack length increases are shown in Figure 4. In the controlled environment (Figure 4a), the impedance magnitude increases over the entire frequency range as the crack length is increased. In the ambient condition (Figure 4b and 4c), the impedance measurements in the low- to mid-frequency range were influenced by temperature and humidity variations and the curves corresponding to crack lengths of 150-250 mm cross each other (more visible in Figure 4c). This effect is clearer in Figure 5 and is discussed further below. However, the measurements in the mid- to high-frequency range were much less sensitive to environmental effects.

The Nyquist plot, in which the real part of the impedance is plotted against the imaginary part of the impedance, more clearly displays the impedance in the low-mid frequency range because the high-frequency measurements are clustered near the origin. Figure 5 shows a typical set of Nyquist plots for the wedge test at ambient conditions. The radii of the arcs in the Nyquist plot represent the magnitude of measured impedance in the mid-low frequency range. For the test under controlled environmental conditions, the radii of the arcs increased progressively with

the debonded length (Harichandran et al. 2003, Hong 2003). However, for the test at ambient conditions (Figure 5) the radii of the arcs do not progressively increase with the crack length, thereby indicating that there is an interaction between the debonding effect and short-term environmental effects (moisture and temperature). The measured impedance decreased when the crack length grew from 150 to 250 mm due to increasing humidity and then increased as the crack length grew further from 250-400 mm. However, the magnitude of impedance in the high-frequency range progressively increases as the crack is propagated.

Tests on the medium specimens indicated that impedance measurements were most stable in a cold environment. For this reason, the large beam was initially placed outdoors from February to March 2003 with the intent of taking stable measurements at cold temperatures in early spring. However, because of large temperature fluctuations that winter, it was decided that measurements would be taken indoors. The measured impedances from the rebar to the copper tapes for the large beam are about an order of magnitude lower than those for the small specimens. This is believed to be due to the larger sensor surface areas in the beam (reinforcement cage and CFRP sheet).

For the wedge test on the large beam the impedance magnitude decreased at low frequencies as the CFRP debonded length increased. This indicated that humidity and temperature variations were interfering with the effect of CFRP debonding in the low- and mid-frequency regions after the large beam was moved indoors. It is postulated that the concrete dried out in the very cold and dry environment when it was outdoors and began to absorb moisture after it was moved indoors. Because of its large size, the beam is likely to have absorbed moisture gradually over a long period of time. The increased moisture and temperature fluctuations from 18^{o}C to 24^{o}C would explain the reduction in impedance at low frequencies. However, at high frequencies, the

magnitude of the impedance increased with the debonded length of the CFRP, since it is not sensitive to humidity and temperature variations as observed for the medium specimens. The measured impedances at high frequencies are shown in Figure 6.

Equivalent circuit analysis also is effective in studying CFRP debonding. In equivalent circuit analysis, the CPE parameter controls the fitted impedance in the low-frequency region and is therefore sensitive to humidity and temperature variations. However, the capacitance parameters are not overly sensitive to the different environmental conditions. All capacitance parameters decreased as the crack length increased. This is contrary to expectations if the capacitance parameters physically represent different interfaces, since the capacitance due to the rebar/electrolyte interface should be independent of crack length. This behavior illustrates that a purely physical interpretation of the empirical equivalent circuit can be problematic. The (R2, C2) and (R3, C3) parameter pairs can switch from one fit to another since they represent symmetric sub-circuits in the equivalent circuit. Thus, rather than treating the C2 and C3 parameters independently, it is convenient to add them. It was found that the C1, C2+C3, and C1+C2+C3 capacitor combinations from the equivalent circuit analysis all correlate well with the crack length with C1 decreasing from 7.5-1.5 nanofarads and C2+C3 decreasing from 25-5 nanofarads (Hong 2003). However, as described later, the C1+C2+C3 combination is the quantity most stable under short- and long-term environmental exposure.

Figure 7 shows that the sum of all capacitance parameters for the medium specimens subjected to controlled and ambient environmental conditions decreased linearly with increasing crack length. Figure 8 shows the C1+C2+C3 values for the large concrete beam due to CFRP debonding. The C1+C2+C3 values decreased significantly during the initial debonding of the CFRP. The different behaviors in Figures 7 and 8 are attributed to scale effects. Wedge tests on

the medium specimens indicated that the C1+C2+C3 value is a reliable indicator of CFRP debonded area and had a low sample-to-sample variation (Hong 2003). The fact that C1+C2+C3 is relatively insensitive to environmental effects makes it a good indicator of CFRP debonding.

Detecting the Location of Debonded Regions

While impedance measurements between the rebar and external sensors provide a global assessment of the debonded area, they are incapable of revealing the location of debonded regions. However, impedance measurements taken between pairs of internal wire sensors (W_i) can be used to locate debonded regions. Measurements were made between adjacent sensors (such as W1 and W2, W2 and W3 and so on) as the internal crack between the CFRP and concrete was propagated.

Nyquist plots for measurements between internal sensors for a typical medium specimen are shown in Figure 9 when the crack tip was located between the W3 and W4 sensors. The Nyquist plot shows a very clear demarcation between readings for sensor pairs in the bonded and debonded regions. The impedance magnitude is much lower when the pair of sensors used are in the bonded region (W4W5 and W5W6), than when the pair of sensors are in the debonded region (W1W2 and W2W3). When one sensor is in the bonded region and the other in the debonded region (W3W4), the impedance magnitude is in between those for the other two cases. It is postulated that the reason for this distinctive difference in the magnitude of impedance is the path of current flow in each case. When the impedance measurement is made between sensors in the debonded area, current must flow through the concrete, and the impedance is high. On the other hand, when measurements are made between sensors in the bonded area, current probably flows predominantly through the highly conductive CFRP sheet, with charge transfer between the internal sensors and the CFRP sheet, resulting in lower impedances.

While raw impedance measurements are sufficient to detect debonded regions, equivalent circuit analysis also can be used. The effect of debonding on the impedances measured between pairs of internal sensors is best observed with the CPE parameter. The variation of the CPE parameter on the large concrete beam is shown in Figure 10 when the crack tip was between the W2 and W3 sensors. Note that a logarithmic scale is used for the vertical axis. The magnitude of the CPE parameter corresponding to measurements between pairs of sensors in the debonded region is about two orders of magnitude higher than that corresponding to pairs of sensors in the bonded region. Although the α parameter of the CPE was different for measurements between different sensor pairs, it was usually less than 0.5 (often less than 0.2) indicating that the CPE was mainly resistive. This is in agreement with the current flow mechanism postulated earlier.

A narrow debonded region that extends in the longitudinal direction across all internal wire sensors will not be able to be detected by the pairwise measurements because all pairwise measurement will reflect the presence of the debond. However, for a large beam, a narrow debonded region will never extend over the whole beam length and if internal wires are distributed over the entire beam length then there will always be internal sensor pairs outside the debonded region.

Moisture is also likely to have an effect on pairwise measurements. However, since all pairwise measurements are typically taken over a short time interval, moisture will affect all readings in a similar way. Since only relative differences in the pairwise measurements are used to locate the debonded regions, moisture will not affect this identification.

Effect of Short-Term Environmental Conditions

Six small specimens were exposed to relative humidity levels of 30%, 60% and 90% in an environmental chamber while the temperature was maintained at 21^{o}C (70^{o}F). Three were manufactured with chloride (11.0 kg NaCl per cubic meter of concrete) and three without chloride. For

each humidity level the specimens were kept in the chamber for at least one week and their weights were measured daily. Impedance measurements were taken only when moisture absorption had ceased and the weights stabilized. Specimens also were exposed to a temperature of 38^{o}C (100^{o}F) for one week in an oven in which the humidity level could not be controlled, and impedance measurements were taken while the specimens remained in the oven.

Figure 11 shows typical impedance spectra measured from the rebar to an external sensor over the entire frequency range for different humidity and temperature levels for a specimen without chloride. Although increasing temperature decreases the impedance measurements over the entire frequency range, they have a significant influence only in the mid-and low-frequency regions. The lower impedance at low-frequencies for specimens in the oven is either due to the increased moisture that might have been present inside the oven at the high temperature or due to a faster rate of diffusion at the higher temperature. Unfortunately the humidity meter could not be exposed to the environment inside the oven and hence the humidity was not measured. Different humidity levels affect the impedance at low frequencies because the amount of pore fluid in the concrete influences the rate of ion diffusion. At high frequencies the impedance is governed by the kinetics of the charge transfer processes at the electrode-electrolyte interface which is not influenced significantly by the moisture content.

In equivalent circuit analysis, the CPE parameter controls the fitted impedance in the low-frequency region and is therefore sensitive to humidity and temperature variations. However, the capacitance parameters are not very sensitive to the different environmental conditions. Figure 12 shows the variation of the sum of all capacitance parameters (C1+C2+C3) from the equivalent circuit analysis at the various humidity and temperature levels for the three specimens without chloride. This measure is considerably different for specimens in the oven (100^{o}F), and also

shows a noticeable change for specimen 3 at 90% relative humidity. However, in general this measure is somewhat insensitive to changes in humidity.

The lack of sensitivity of C1+C2+C3 to humidity changes might appear counter-intuitive. For parallel plate capacitors, the capacitance is dependent on the electrical permittivity of the dielectric as shown in Eq. (6). With moisture uptake, the permittivity of the dielectric should change thereby causing a change in the capacitance. Davis et al. (1999) were able to correlate the moisture uptake into the adhesive with capacitance when studying metal/FRP bonds. For the concrete specimens, however, the concrete is more like an electrolyte than a dielectric, and moisture absorption by the concrete only changes the electrolyte resistance. The dielectric adjacent to the FRP is more likely to be the epoxy adhesive, which will not absorb a significant amount of moisture due to humidity changes in the environment. More aggressive wetting of the specimen would be required to cause significant moisture uptake by the epoxy adhesive.

Effect of Long-term Environmental Conditions

Three sets, each containing three small specimens, were exposed to: (1) 300 cycles of freeze-thaw using the ASTM C666 Procedure B; (2) 300 cycles of wetting and drying with two hours of immersion in water and ten hours of drying during each cycle; and (3) 21 days of accelerated corrosion using a 12V power supply with specimens immersed in a 2% sodium chloride solution for one hour and exposed to air for 23 hours each day. The specimens used in the accelerated corrosion test contained a second rebar near the upper surface that was used as the cathode, while the bar near the bottom was the anode subjected to corrosion. The corroded anode was used as the electrode for EIS. Baiyasi and Harichandran (2001) used this corrosion test previously. Based on the total current over the 21 days and use of Faraday's Law, the total steel loss was

estimated to be about 13g for each specimen. This represents an average corrosion depth of 0.45 mm (3.6% loss) over the bar (Hong 2003).

Figure 13 shows typical impedance spectra measured from the rebar to an external sensor before and after the three different long-term environmental exposures. Long-term environmental conditions generally tend to deteriorate the concrete and increase the width and density of microcracks. This increases the mobility of ions within the concrete and hence reduces the magnitude of impedance. The results indicate that the reduction in impedance is most significant in the low- to mid-frequency regions where diffusion is the primary mode of conductance. Figure 14 shows the variation of the sum of the capacitance parameters (C1+C2+C3) from the equivalent circuit analysis before and after the different long-term environmental conditions for a typical specimen. It is apparent that the high-frequency impedance measurements and the C1+C2+C3 parameter are insensitive to the long-term environmental conditions.

Recommendations for Field Implementation

In the proposed EIS technique, the impedance of an electrochemical cell is measured between two electrode sensors. These are the reinforcing bar, internal sensors and external sensors. Internal sensors (W_i) are installed before the CFRP sheet is applied and external sensors (C_i) are installed on the outside of the last CFRP sheet before the protective epoxy layer is applied. Internal sensors cannot be installed in beams that have already been retrofitted with CFRP. Internal sensors consist of 0.625 mm diameter stainless steel wire installed in grooves. These installations can be done both for prefabricated and cast-in-place beams, although it is much easier to install the sensors in prefabricated beams. Wiring from the sensors need to be collected and routed to a junction box to which a portable potentiostat could be connected when impedance measurements are to be taken.

Impedance measured between a rebar and the external copper tape sensors are most effective for assessment of the total debonded area. Only one or two external sensors are needed for a large beam. Therefore, using just a few measurements the global state of the bond can be assessed. Measurements must be taken once or twice a year from the time the sensors are installed, and subsequent measurements must be compared with initial measurements. Care must be exercised to account for variations in measurements that are caused by variations in environmental conditions when measurement are taken by using the sum of the capacitance parameters of the equivalent circuit or by only using high-frequency measurements. Measurements should not be taken on very hot summer days when temperatures may approach 100°F. As shown in Figure 8, a significant change in the C1+C2+C3 parameters is observed when only about 100 mm of the CFRP is debonded. Once CFRP debonding is detected using the measurements from a rebar to external sensors, measurements can be taken between pairs of internal sensors to locate the debonded regions for performing repairs. One set of impedance measurements from 100,000 Hz to 0.1 Hz takes about five minutes.

The installation of the wire sensors may appear tedious in practice. However, this is true of almost any structural health monitoring system that employs sensors. While the initial labor cost for the installation may be high, the stainless steel wire sensors are extremely inexpensive and the long-term monitoring cost is also modest.

Conclusions

Electrochemical impedance spectroscopy (EIS) is used for nondestructive evaluation (NDE) of carbon fiber reinforced polymer (CFRP) debonding in concrete beams strengthened with CFRP sheets. Sensor elements (electrodes) consisted of: (a) copper tape with a conductive adhesive applied to the outside of the CFRP prior to application of the epoxy; (b) stainless steel

wire placed in grooves on the bottom face of the concrete; and (c) a reinforcing bar. Impedance measurements were taken between pairs of sensors using a potentiostat. An equivalent circuit was fitted to each measured impedance spectrum and the circuit parameters were estimated. Variations in the measured impedance spectra and the equivalent circuit parameters due to different environmental conditions and debonding of the CFRP sheet were studied in controlled and ambient conditions.

Impedance measurements taken between a rebar and external copper tape sensors can be used to assess the total debonded area. The sum of the capacitance parameters in the equivalent circuit correlate well with the debonded area and is not sensitive to environmental factors. Impedance measurements taken between pairs of internal wire sensors reveal the location of debonded regions. The EIS-based sensor technology shows promise for inexpensive and effective NDE of concrete structures strengthened with CFRP.

Acknowledgments

The Michigan State Department of Transportation (MDOT) funded this research. The project manager was Roger D. Till. Dr. Guy Davis from DACCO SCI Inc., Columbia, Maryland, shared with the authors the basic techniques he developed for the use of EIS for NDE. Dr. Ahmed Alostaz, presently with the Department of Civil Engineering, University of Mississippi, Oxford, Mississippi, was involved in this project during the early stages.

References

Akuthota, B., Hughes, D., Zoughi, R., Myers, J.J. and Nanni, A. (2004). "Near-field microwave detection of disbond in carbon fiber reinforced polymer composites used for strengthening

cement-based structures and disbond repair verification." *Journal of Materials in Civil Engineering*, ASCE, 16(6), 540-546.

Baiyasi, I. M., and Harichandran, R. S. (2001). "Corrosion and wrap strains in concrete bridge columns repaired with FRP wraps." *Proceedings (CD-ROM), 80th Annual Meeting of the Transportation Research Board*, Washington, D.C., Paper No. 01-2609, 11 pp.

Buyukozturk, O., and Hearing, B. (1998). "Failure behavior of precracked concrete beams retrofitted with FRP." *Journal of Composites for Construction*, Vol. 2 (3), August, 138-144.

Davis, G.D., Krebs, L.A., Drzal, L.T., Rich, M.J., and Askeland, P. (2000). "Electrochemical sensors for nondestructive evaluation of adhesive bonds." *Journal of Adhesion*, Vol. 72, 335-358.

Davis, G.D., Rich, M. J., Harichandran, R.S., Drzal, L. T., Mase, T., and Al-Ostaz, A. (2003). "Development of an electrochemical impedance sensor to monitor delamination and moisture uptake in CFRP-reinforced concrete structures." *Proceedings, 81st Annual Meeting of the Transportation Research Board (CD-ROM)*, National Research Council, Washington, D.C., Paper No. 03-2392.

Davis, G.D., Dacres, C.M., and Krebs, L.A. (1999). "In-situ sensor to detect moisture intrusion and degradation of coatings, composites, and adhesive bonds." *Proc., Tri-Services Conference on Corrosion*, Myrtle Beach, South Carolina.

Gamry Instruments. (2005). "Electrochemical impedance spectroscopy theory: a primer." <http://www.gamry.com/App_Notes/EIS_Primer/EIS_Primer.htm> (February 19, 2005).

Gamry Instruments. (1997). "Redefining electrochemical measurements." <http://www.gamry.com/Homepage/Index.html> (October 20, 2003).

Harichandran, R.S., Hong, S., Al-Ostaz, A., and Davis, G.D. (2003). "NDE of bond integrity in concrete structures strengthened with carbon FRP using EIS." *Proceedings, 1st International Conference on Structural Health Monitoring and Intelligent Infrastructure*, Tokyo, Japan, November, 1183-1190.

Hong, S. (2003). "Electrochemical impedance spectroscopy based sensors for NDE of CFRP/concrete bond in beams." MS Thesis, Dept. of Civil and Environmental Engineering, Michigan State University, East Lansing, Michigan.

Karbhari, V. M., and Zhao, L. (2000). "Use of composites for 21st century civil infrastructure." *Computer Method in Applied Mechanics and Engineering,* 185(2-4), 433-454.

Kendig, M.W., and Scully, J.R. (1989). "Basic aspects of the application of electrochemical impedance for the life prediction of organic coatings on metals." *Corrosion J.*, Vol. 45, April.

Mirmiran, A. and Wei, Y. (2001). "Damage assessment of FRP-encased concrete using ultrasonic pulse velocity." *Journal of Engineering Mechanics*, ASCE, 127(2), 126-135.

Nguyen, D.M., Chan, T.K., and Cheong, H.K. (2001). "Brittle failure and bond development length of CFRP-concrete beams." *Journal of Composites for Construction*, 5(1), 12-17.

Rahimi, H., and Hutchinson, A. (2001). "Concrete beams strengthened with externally bonded FRP plates." *Journal of Composites for Construction*, 5(1), 44-56.

List of Figures

Figure 12: Variation of C1+C2+C3 with humidity and temperature (legend: F-temperature in °F, H-relative humidity)

Figure 13: Typical impedance measurements before and after 21 days of accelerated corrosion of the rebar, and 300 cycles of freezing/thawing and wetting/drying (legend identifies the time of measurement and the exposure: B-before, A-after, C-corrosion, FT-freeze/thaw, WD-wet/dry)

Figure 14: Variation of C1+C2+C3 before and after 21 days of accelerated corrosion of the re-bar, and 300 cycles of freezing/thawing and wetting/drying

Table 1. Experimental matrix

Test Type	**Specimen Size**	**Number of Specimens**
Temperature	Small	3 without chloride, 3 with chloride
Humidity	Small	3 without chloride, 3 with chloride
Freeze-thaw	Small	3 with chloride
Wet-dry	Small	3 with chloride
Corrosion	Small	3 without chloride
CFRP debonding	Medium	3 with chloride in controlled env. 3 with chloride in ambient env.
CFRP debonding	Large	1 without chloride

Table 2. Initial values of equivalent circuit element parameters

Parameter	Rebar to External		Internal to Internal	
	Low	High	Low	High
R1 (ohm)	1.0E+03	1.0E+07	1.0E+08	1.0E+08
C1 (Farad)	1.0E-07	1.0E-08	1.0E-08	1.0E-10
R2 (ohm)	1.0E+01	1.0E+03	1.0E+04	1.0E+04
C2 (Farad)	1.0E-07	1.0E-08	1.0E-08	1.0E-10
R3 (ohm)	1.0E+01	1.0E+04	1.0E+06	1.0E+06
C3 (Farad)	1.0E-07	1.0E-08	1.0E-08	1.0E-10
CPE: A (Farad)	1.0E+06	1.0E+07	1.0E+08	1.0E+08
CPE: α	0.6	0.6	0.6	0.1

(a)

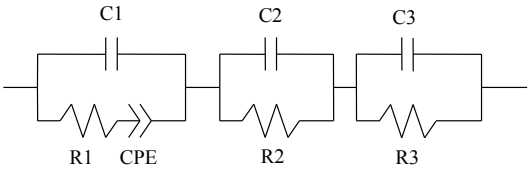
C1
C2
C3
R1
CPE
R2
R3

(b)

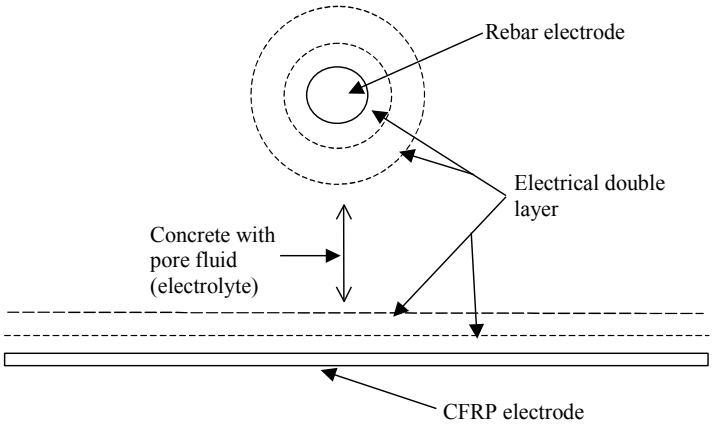
Rebar electrode
Electrical double layer
Concrete with pore fluid (electrolyte)
CFRP electrode

Fig. 1

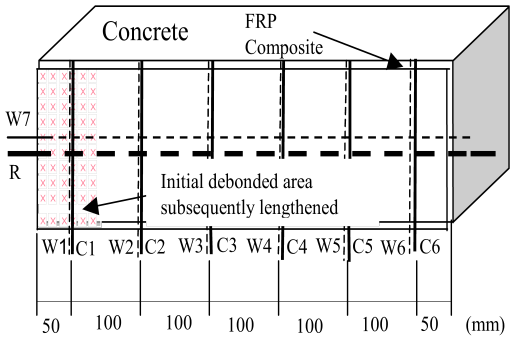

C_i are external sensors (solid lines)

W_i are internal sensors (dashed lines)

Fig. 2

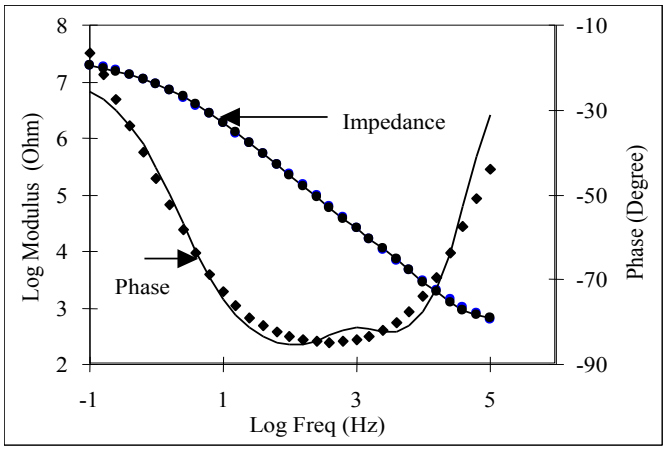
8
7
6
5
4
3
2
-10
-30
-50
-70
-90
-1
1
3
5
Log Modulus (Ohm)
Phase (Degree)
Log Freq (Hz)
Impedance
Phase

Fig. 3

(a)

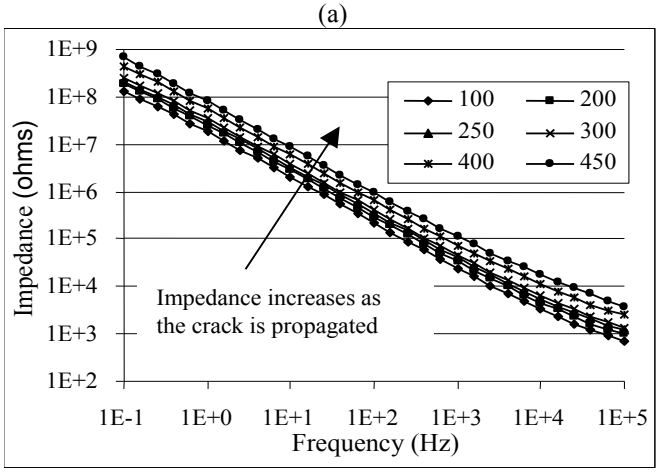
1E+9
1E+8
1E+7
1E+6
1E+5
1E+4
1E+3
1E+2
Impedance (ohms)
100
200
250
300
400
450
Impedance increases as
the crack is propagated
1E-1
1E+0
1E+1
1E+2
1E+3
1E+4
1E+5
Frequency (Hz)

(b)

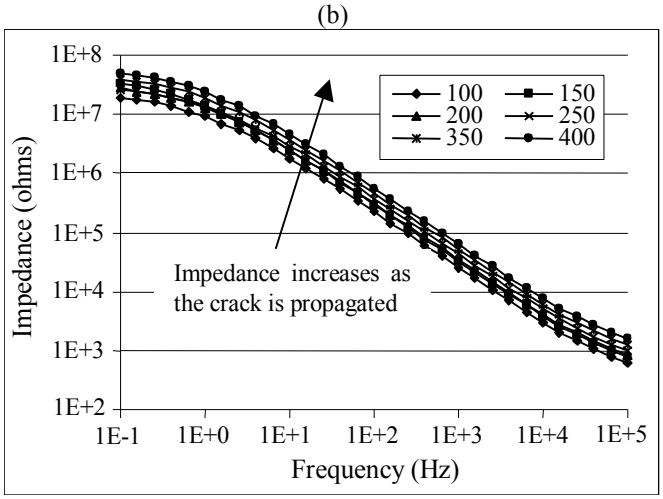
1E+8
1E+7
1E+6
1E+5
1E+4
1E+3
1E+2
Impedance (ohms)
100
150
200
250
350
400
Impedance increases as
the crack is propagated
1E-1
1E+0
1E+1
1E+2
1E+3
1E+4
1E+5
Frequency (Hz)

(c)

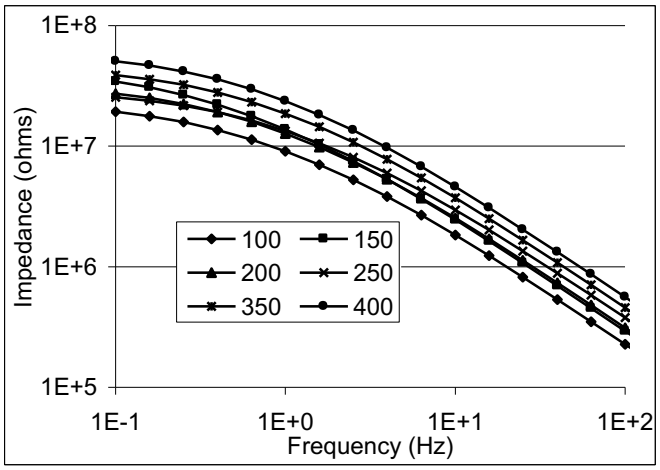
1E+8
1E+7
1E+6
1E+5
Impedance (ohms)
100
150
200
250
350
400
1E-1
1E+0
1E+1
1E+2
Frequency (Hz)

Fig. 4

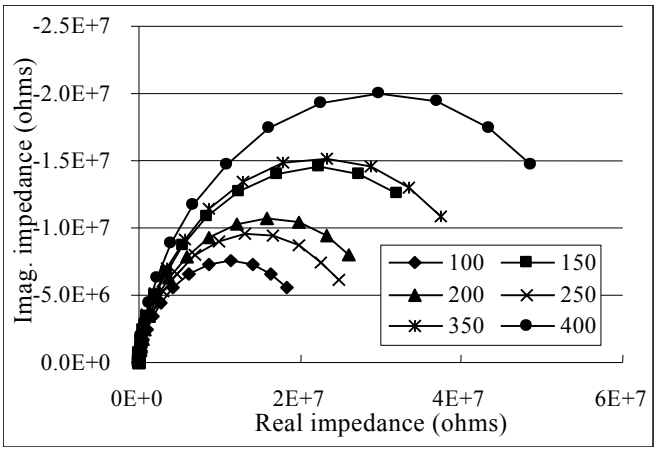
-2.5E+7
-2.0E+7
-1.5E+7
-1.0E+7
-5.0E+6
0.0E+0
Imag. impedance (ohms)
0E+0
2E+7
4E+7
6E+7
Real impedance (ohms)
100
150
200
250
350
400

Fig. 5

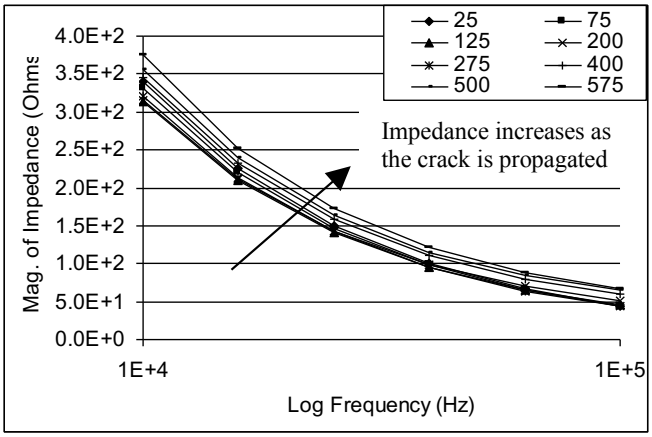
4.0E+2
3.5E+2
3.0E+2
2.5E+2
2.0E+2
1.5E+2
1.0E+2
5.0E+1
0.0E+0
Mag. of Impedance (Ohms
1E+4
1E+5
Log Frequency (Hz)
25
75
125
200
275
400
500
575
Impedance increases as
the crack is propagated

Fig. 6

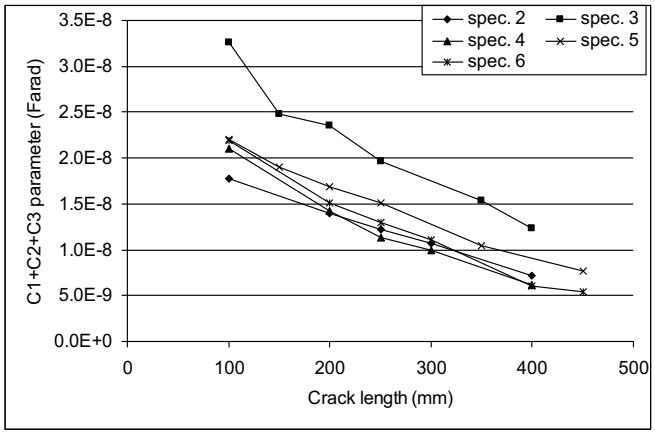
spec. 2
spec. 3
spec. 4
spec. 5
spec. 6
C1+C2+C3 parameter (Farad)
3.5E-8
3.0E-8
2.5E-8
2.0E-8
1.5E-8
1.0E-8
5.0E-9
0.0E+0
0
100
200
300
400
500
Crack length (mm)

Fig. 7

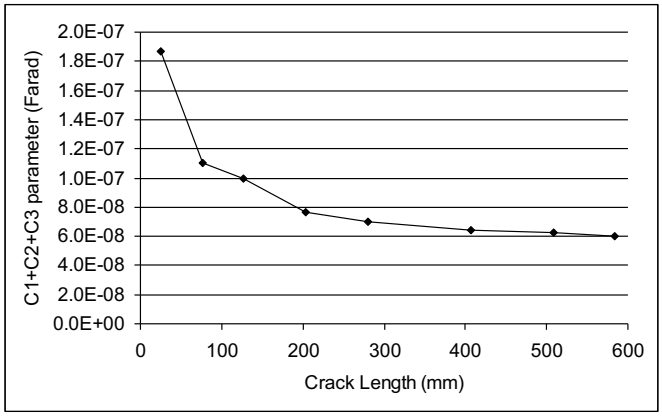
C1+C2+C3 parameter (Farad)
2.0E-07
1.8E-07
1.6E-07
1.4E-07
1.2E-07
1.0E-07
8.0E-08
6.0E-08
4.0E-08
2.0E-08
0.0E+00
0
100
200
300
400
500
600
Crack Length (mm)

Fig. 8

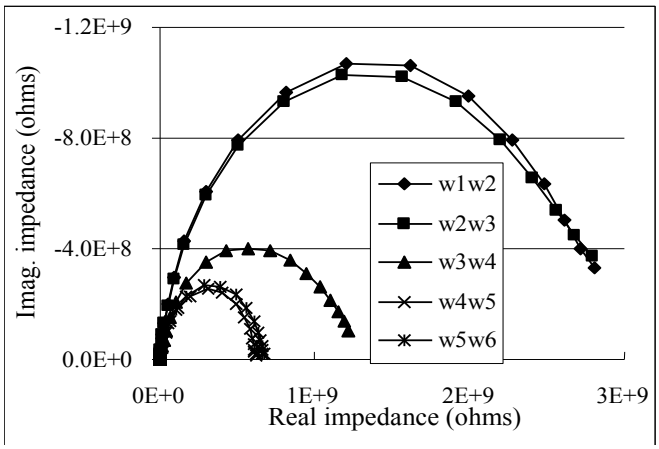
-1.2E+9
-8.0E+8
-4.0E+8
0.0E+0
Imag. impedance (ohms)
0E+0
1E+9
2E+9
3E+9
Real impedance (ohms)
w1w2
w2w3
w3w4
w4w5
w5w6

Fig. 9

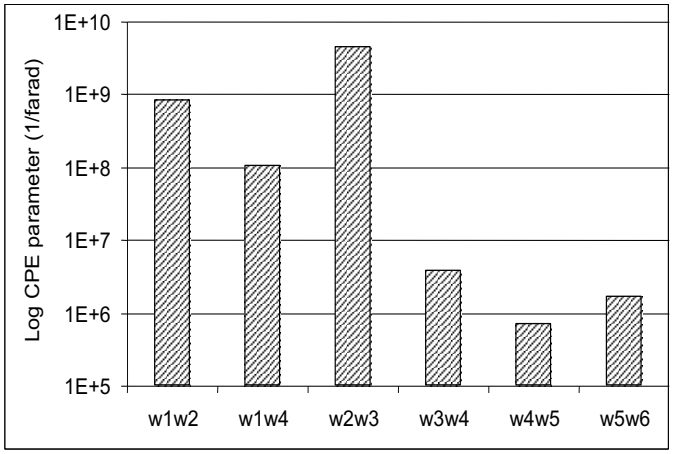
1E+10
1E+9
1E+8
1E+7
1E+6
1E+5
Log CPE parameter (1/farad)
w1w2
w1w4
w2w3
w3w4
w4w5
w5w6

Fig. 10

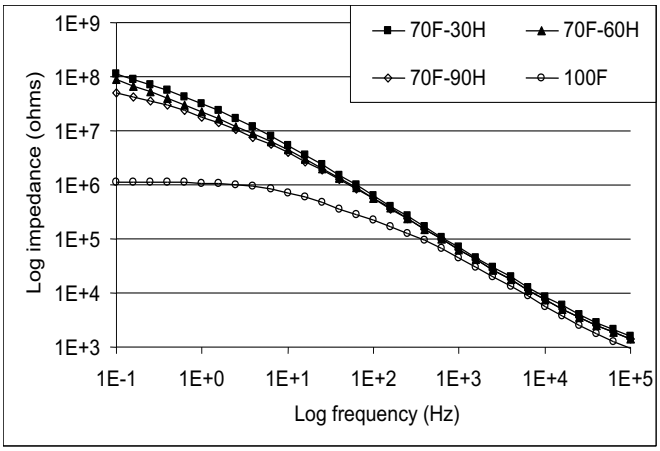
70F-30H
70F-60H
70F-90H
100F
Log impedance (ohms)
1E+9
1E+8
1E+7
1E+6
1E+5
1E+4
1E+3
1E-1
1E+0
1E+1
1E+2
1E+3
1E+4
1E+5
Log frequency (Hz)

Fig. 11

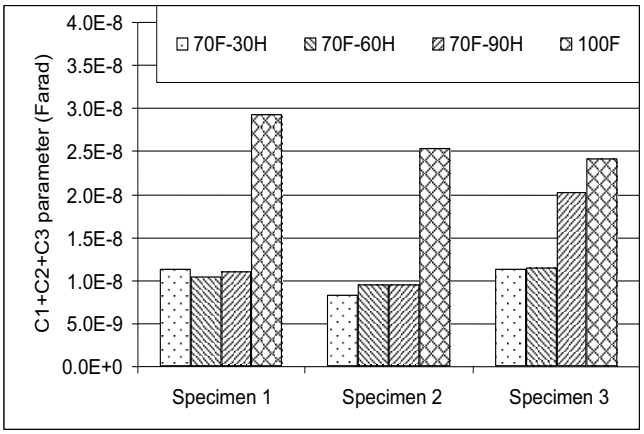
70F-30H
70F-60H
70F-90H
100F
C1+C2+C3 parameter (Farad)
4.0E-8
3.5E-8
3.0E-8
2.5E-8
2.0E-8
1.5E-8
1.0E-8
5.0E-9
0.0E+0
Specimen 1
Specimen 2
Specimen 3

Fig. 12

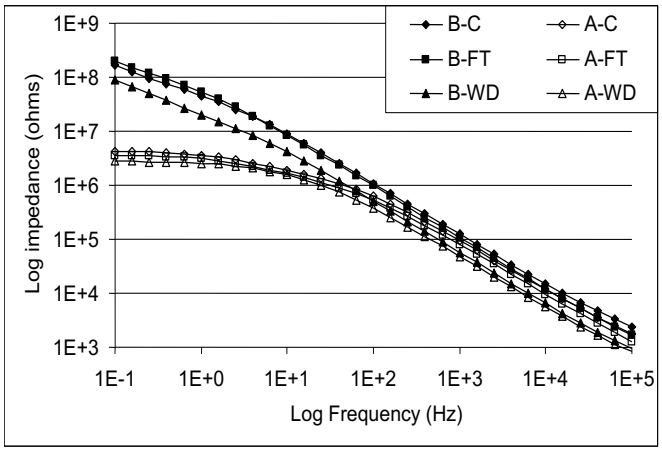
B-C
A-C
B-FT
A-FT
B-WD
A-WD
1E+9
1E+8
1E+7
1E+6
1E+5
1E+4
1E+3
Log impedance (ohms)
1E-1
1E+0
1E+1
1E+2
1E+3
1E+4
1E+5
Log Frequency (Hz)

Fig. 13

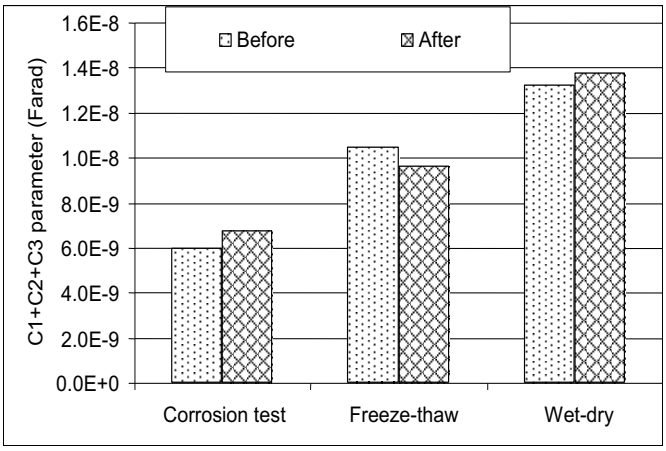
Before
After
1.6E-8
1.4E-8
1.2E-8
1.0E-8
8.0E-9
6.0E-9
4.0E-9
2.0E-9
0.0E+0
C1+C2+C3 parameter (Farad)
Corrosion test
Freeze-thaw
Wet-dry

Fig. 14